Electronic Supplementary Material (ESI) for Lab on a Chip.

Supplemental Figures

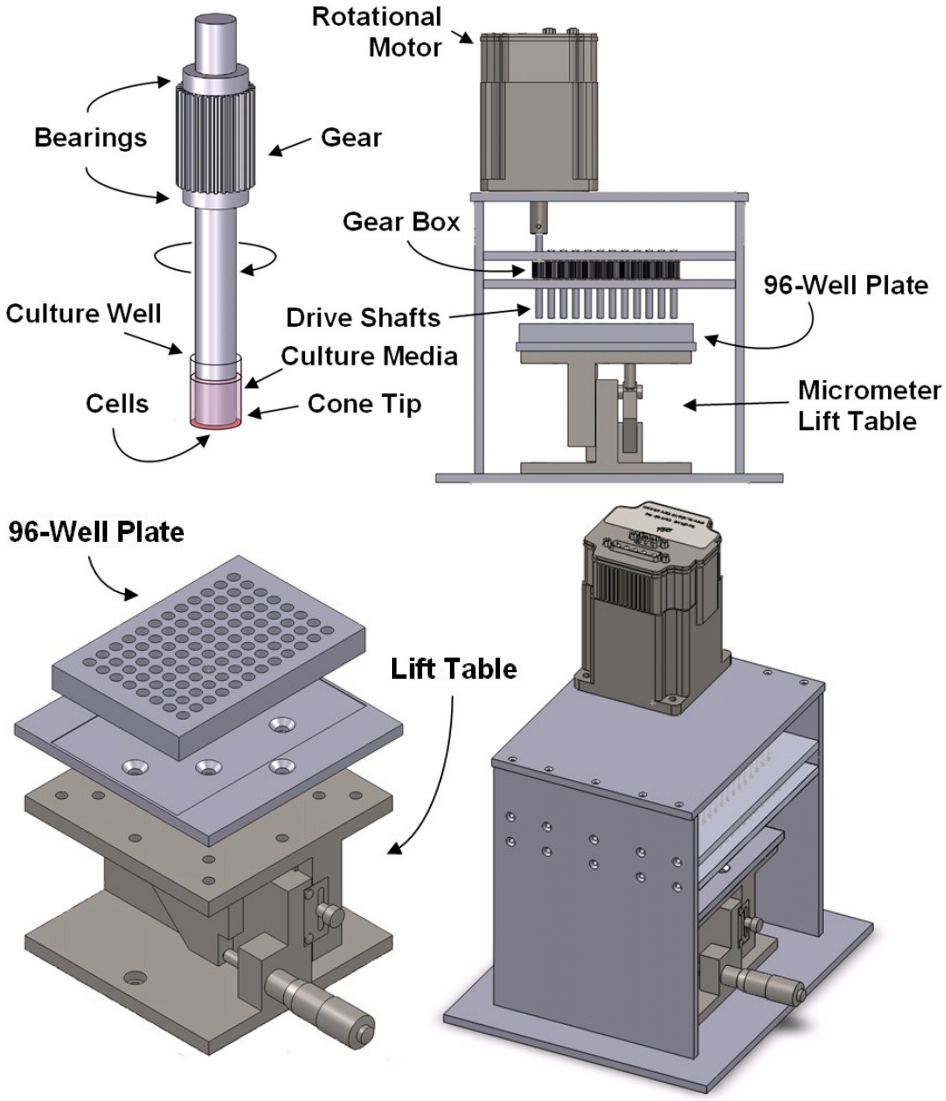

Supplementary Figure S1. Mechanical design of the HT-CAP device. A single shaft is linked into a 96-shaft gearbox through precision gears. A lift table allows precise vertical position of the well plate relative to the cone-tipped shafts.

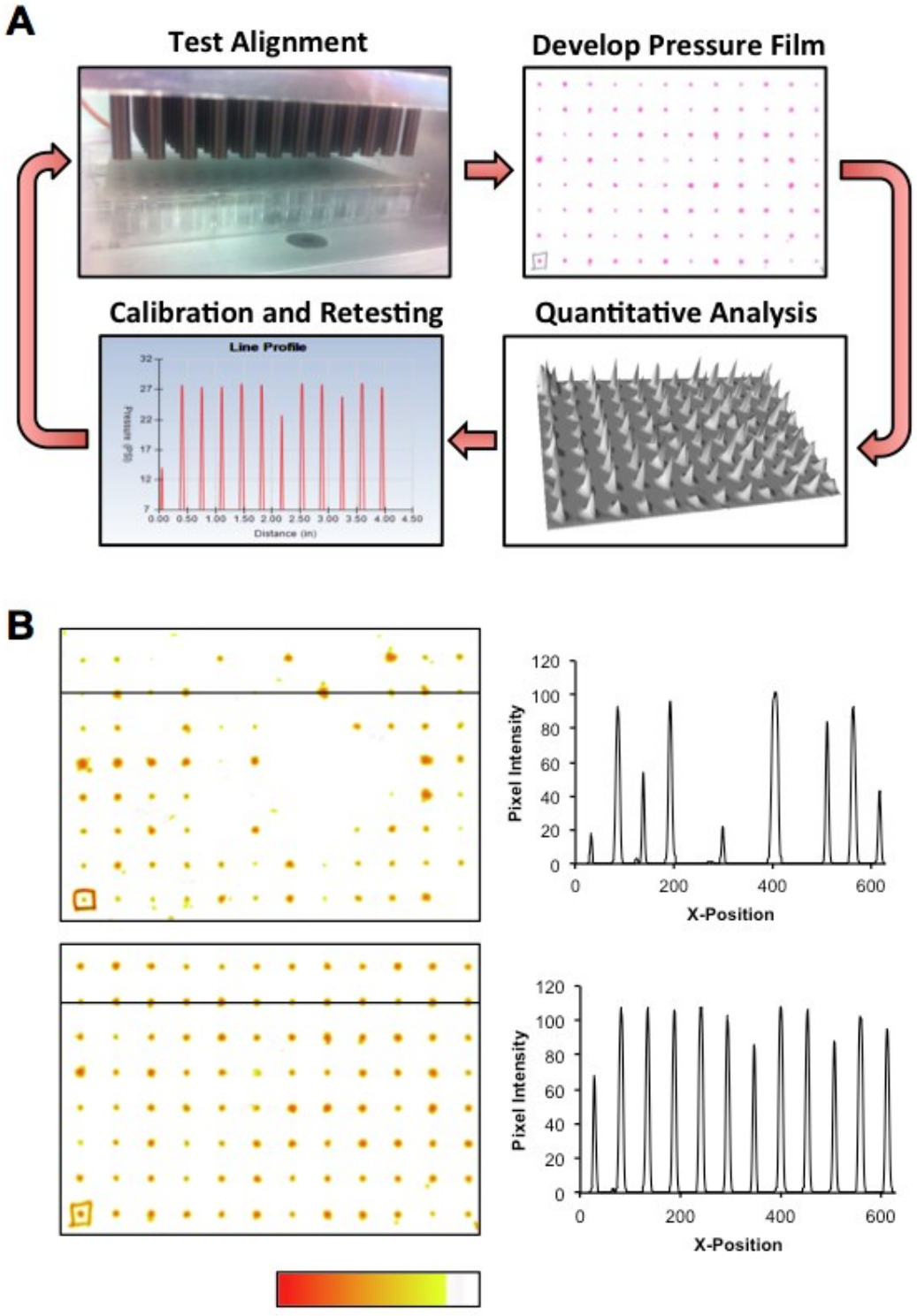

Supplementary Figure S2. Alignment of the cone tips using pressure sensitive film. (A) Overall procedure for alignment of the cones. (B) Top left: pressure film when the shafts are poorly aligned. Top right: a line scan of intensity along the line shown in the diagram. Bottom left: pressure film during alignment process as the alignment is progressively improved. Bottom right: intensity along line scan when the shafts are more aligned. The alignment process was continued until the pressure for all of the cones were identical on the pressure file.

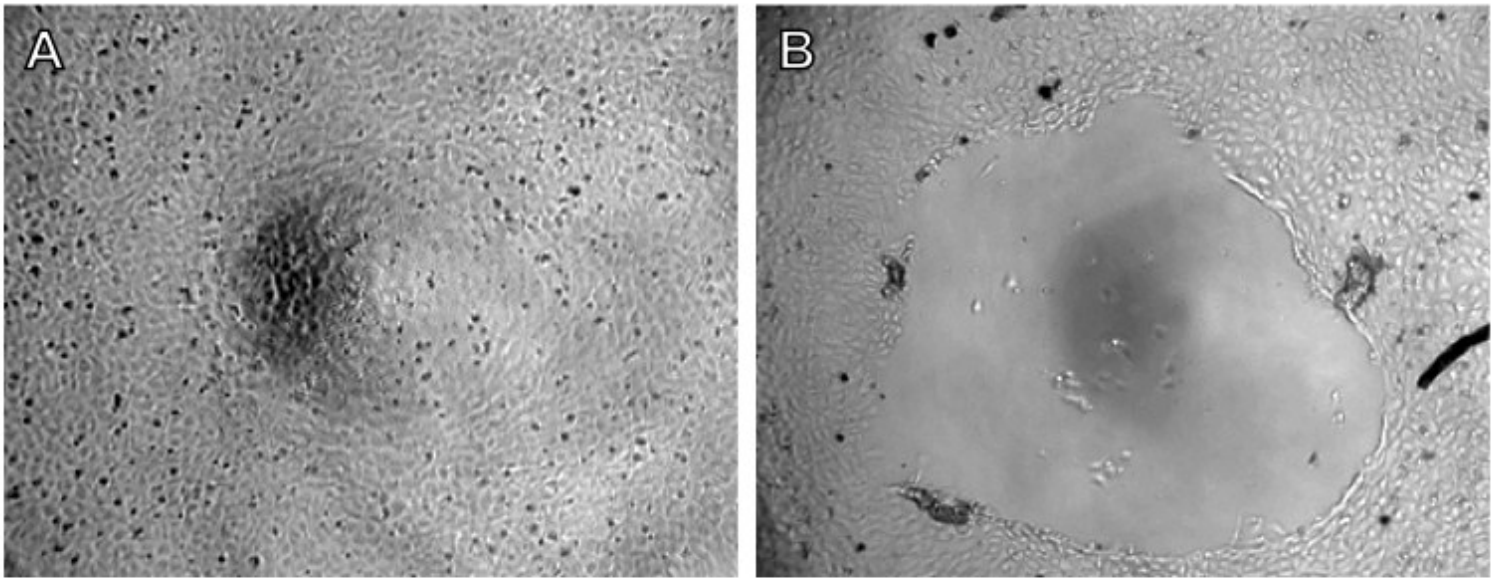

Supplementary Figure S3. Adjustment of the system to account for cell thickness. (A) System height set in final configuration. (B) System height set too low during calibration leading to denudation of central region under the cone tip.

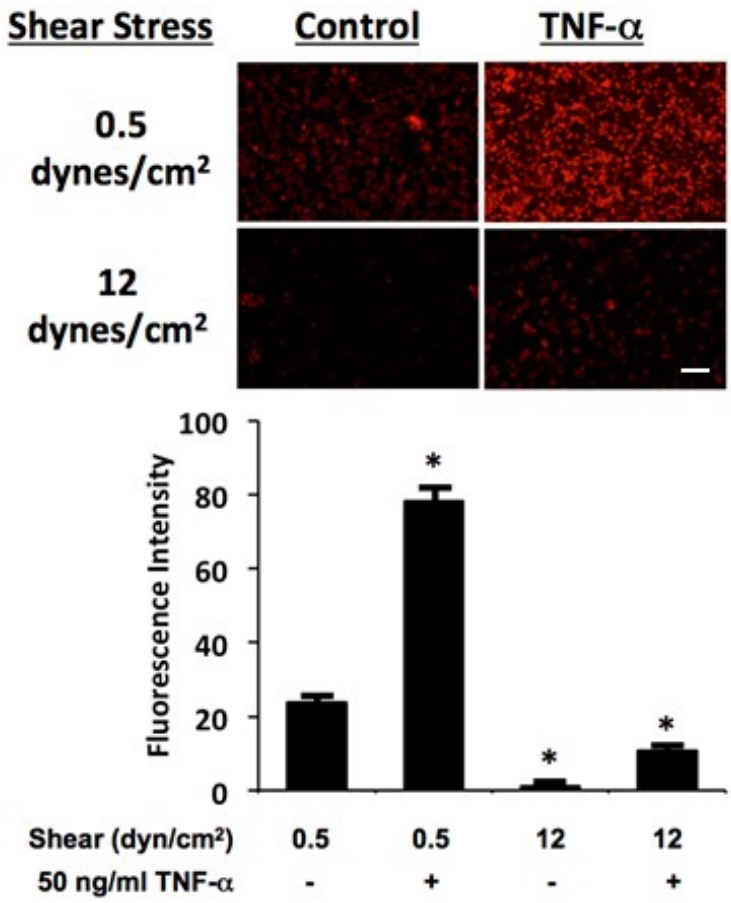

Supplementary Figure S4. Initial validation of the device using adhesion of THP-1 cells (red). Endothelial cells were treated with TNF-α for 1 hour and then fluorescently labeled THP-1 cells were flowed over the endothelial cells for 10 minutes at the shear stress indicated. Bar = 100μm.

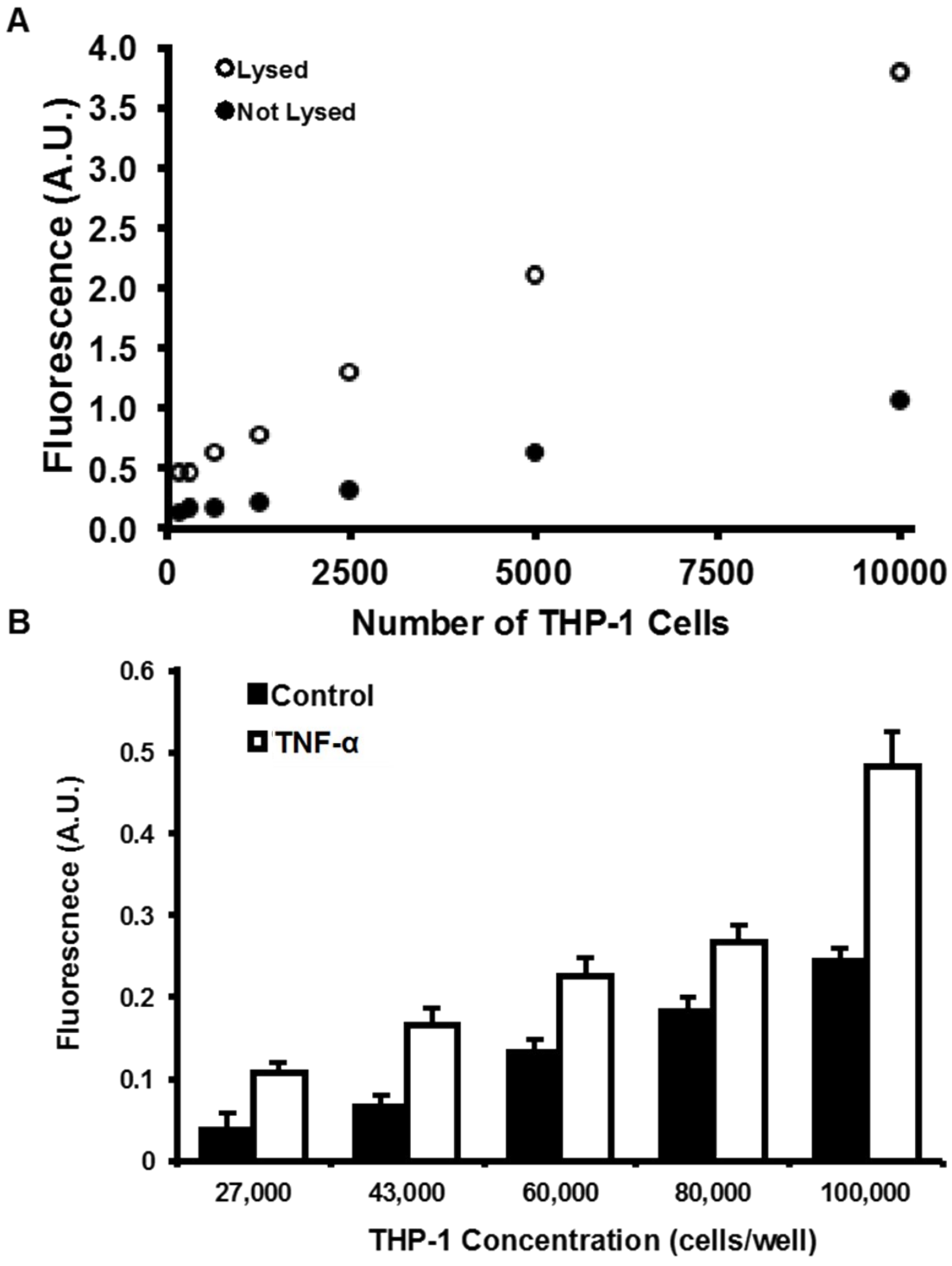

Supplementary Figure S5. Pictures of the high throughput shear stress device. (A) Performance of the assay with varying numbers of cells with and without lysis. (B) THP-1 cell adhesion with varying numbers of cells to optimize the assay signal.

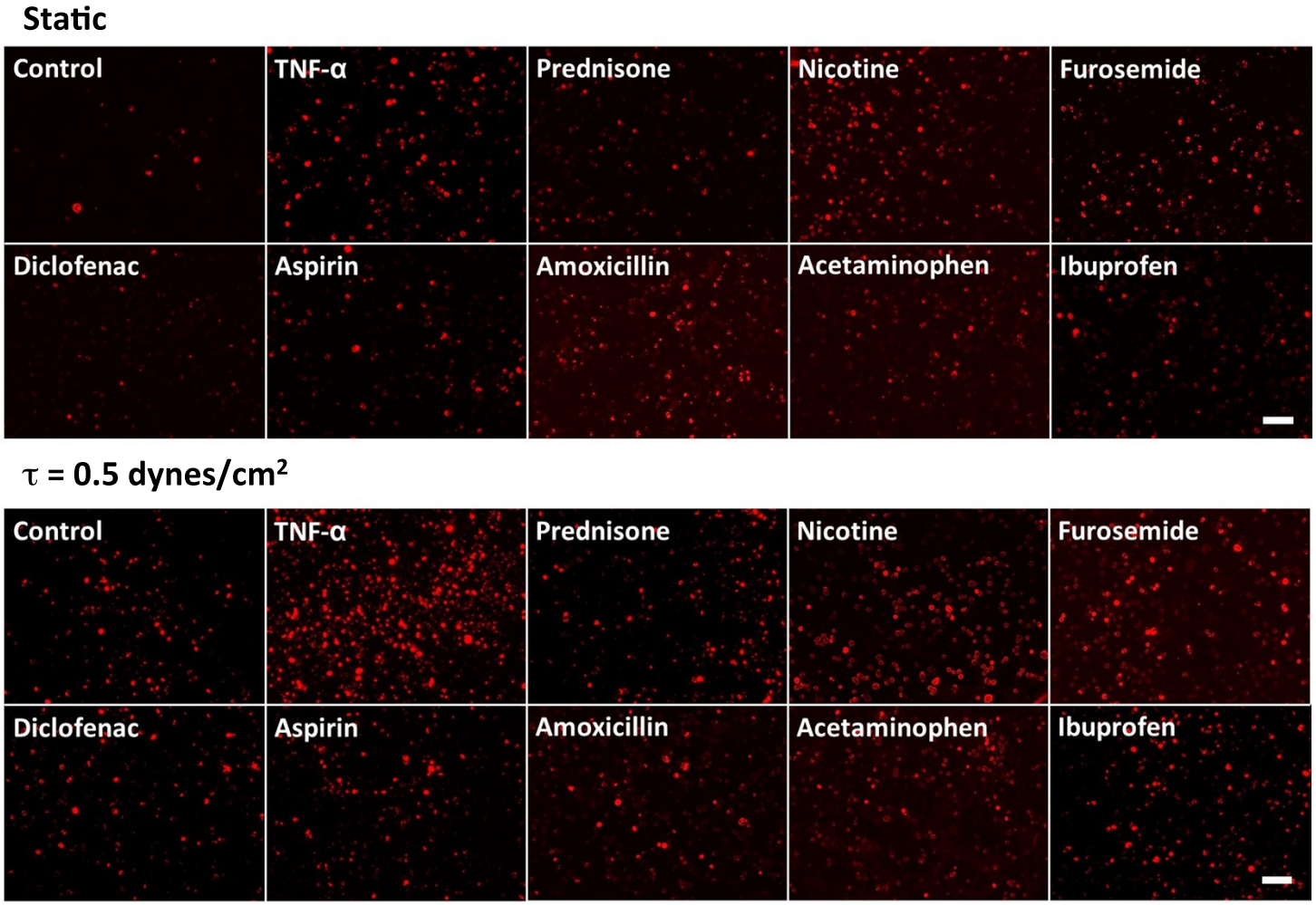

Supplementary Figure S6. Adhesion of THP-1 cells to TNF-α stimulated endothelial cells. Endothelial cells were grown to confluence and treated with 10 ng/ml of TNF-α for 4 hours. Endothelial cells were treated with the compounds at the concentrations listed in **Table 1** for 1 hour prior to stimulation with TNF-α. The THP-1 cells were added to the endothelial cells and allowed to adhere for 15 minutes under static or flow conditions (0.5 dynes/cm^2) shear stress.

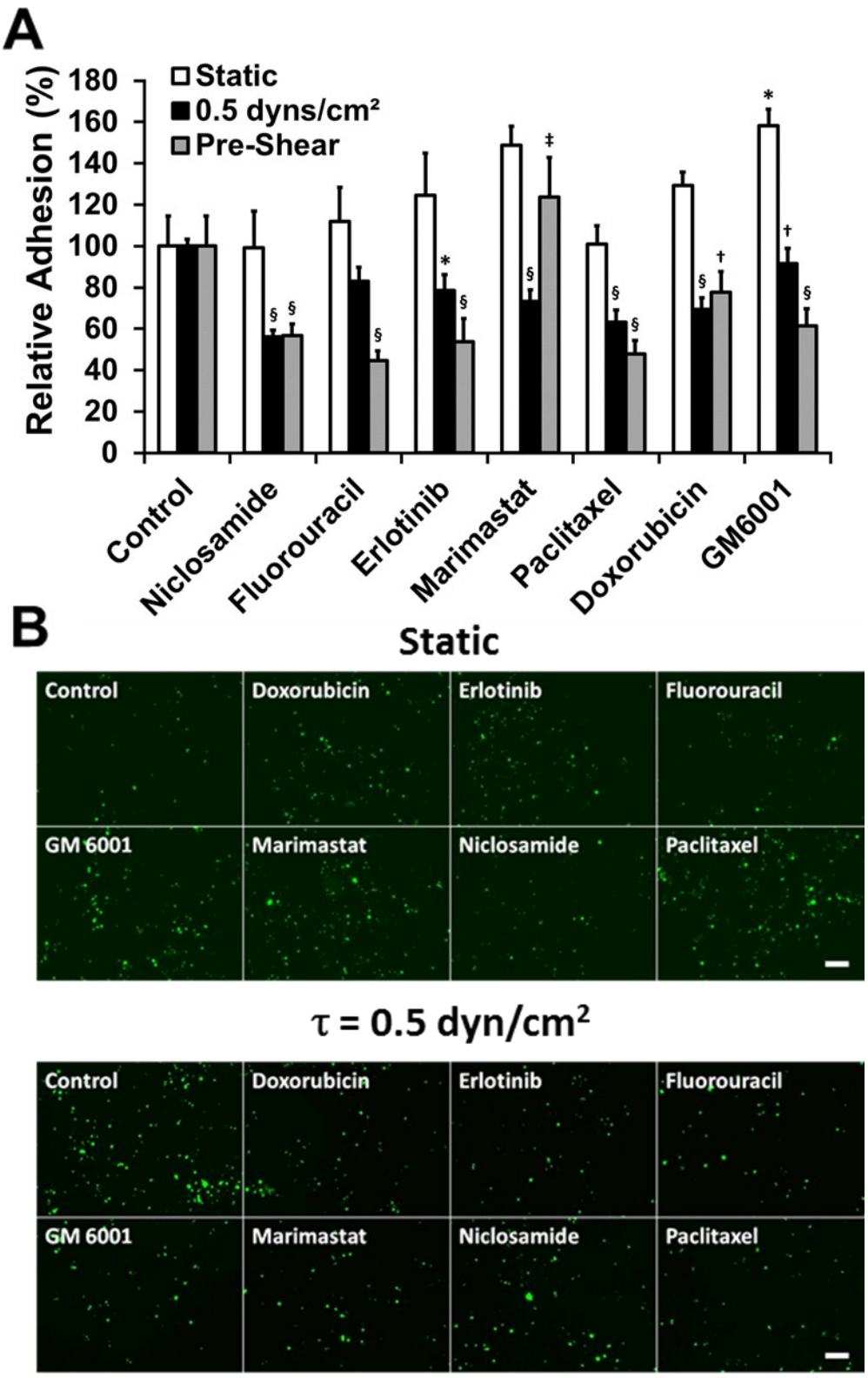

Supplementary Figure S7. Adhesion of colon cancer cells after treatment with chemotherapeutic compounds and compounds that may alter metastasis. HCT-116 cancer cells were grown for 4 hours in the chemotherapeutic agents, fluorescently labeled and trypsinized. After one hour of recovery the cells were used in a static or flow adhesion assay on endothelial cells. The adhesion assay was performed on endothelial cells under static conditions (Static), low shear stress at the start of the assay (0.5 dynes/cm^2) or cells that had been sheared for 8 hours before the assay (Pre-Shear). *$p < 0.05$ treatment versus respective static, shear or pre-sheared control, †$p < 0.05$ shear or pre-sheared versus static within each treatment, ‡$p < 0.05$ shear versus pre-sheared cells within each treatment, § $p < 0.05$ for both treatment versus control for respective shear condition and shear or pre-shear versus static within each treatment. Bar = 100 μm.

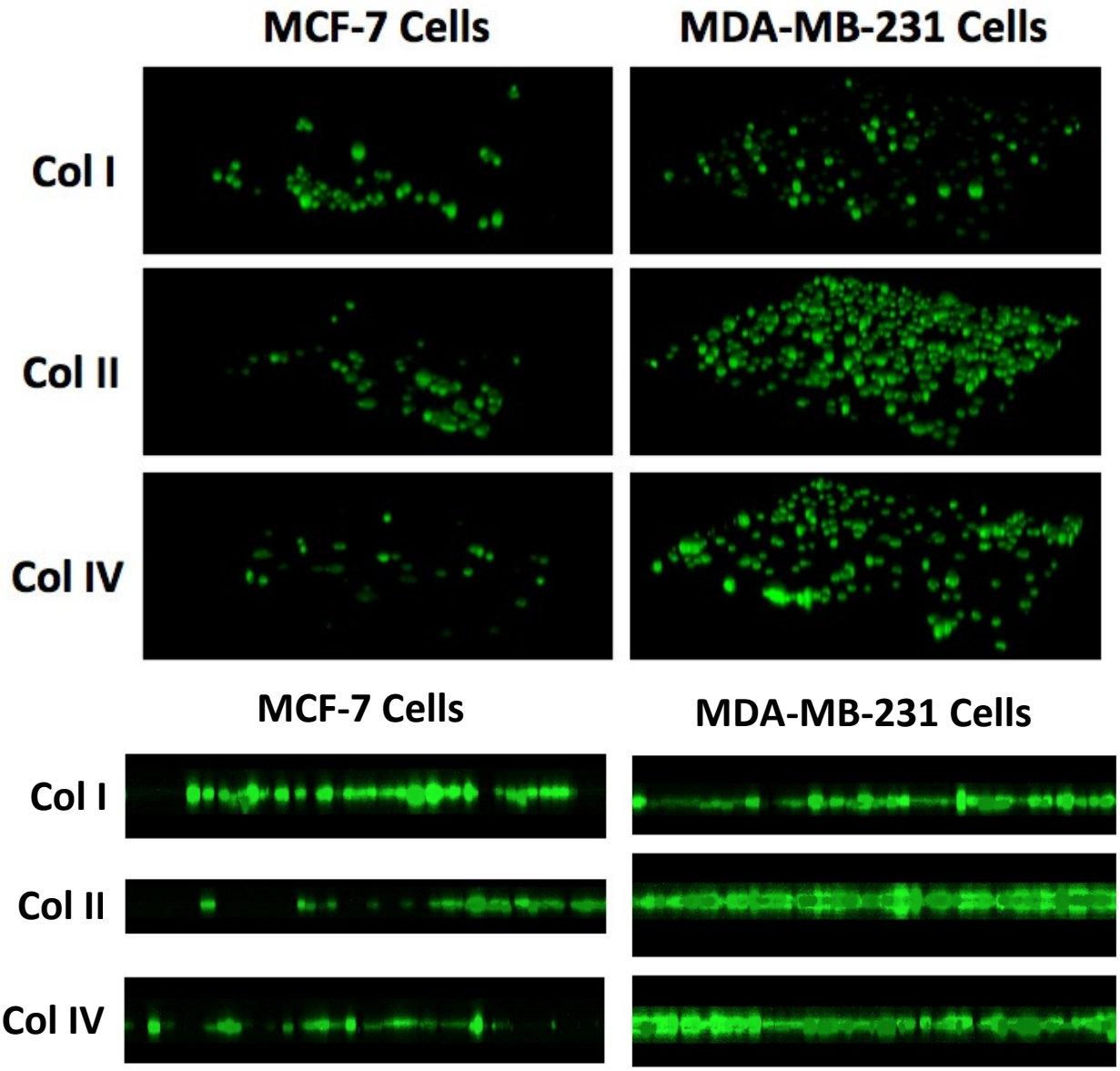

Supplementary Figure S8. Confocal z-stack images of adhered cancer following adhesion to ECM coated surfaces.

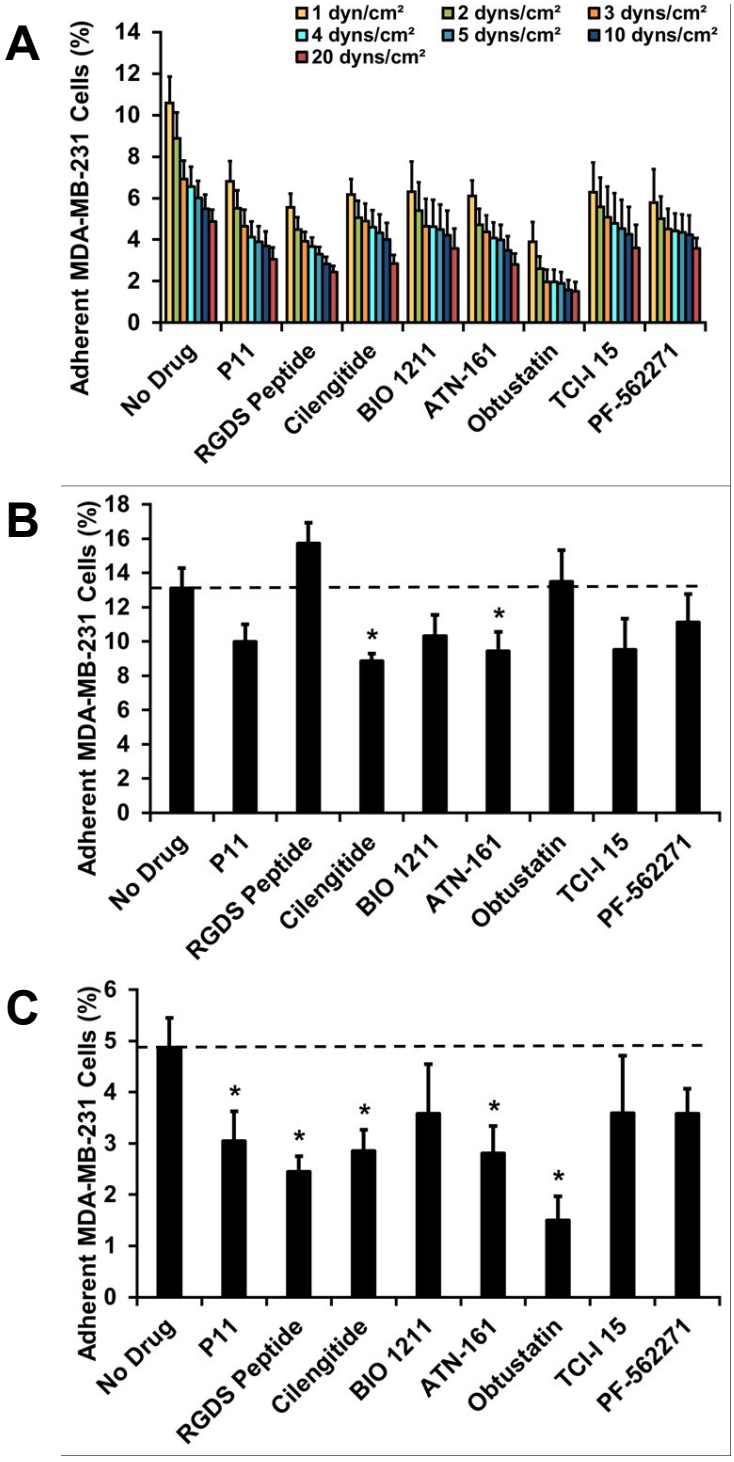

Supplementary Figure S9. Adhesion-deadhesion assay for MDA-MB-231 cancer cells under oscillatory flow. The cancer cells were adhered to TNF-α stimulated endothelial cells under oscillatory flow varying from 1.0 to -1.0 dynes/cm^2 of shear stress for one hour followed by increasing bouts of shear stress up through 20 dynes/cm^2 to detach the cells. Cancer cells were detached from the endothelial cells for 1 minute under each shear stress. (A) Percent of cancer cells remaining attached after application of shear stress. (B) Percent of cancer cells that adhered after 1 hour of oscillatory flow. (C) Percent of cancer remaining after 20 dynes/cm^2 of shear stress. *$p < 0.05$ versus the no drug group.

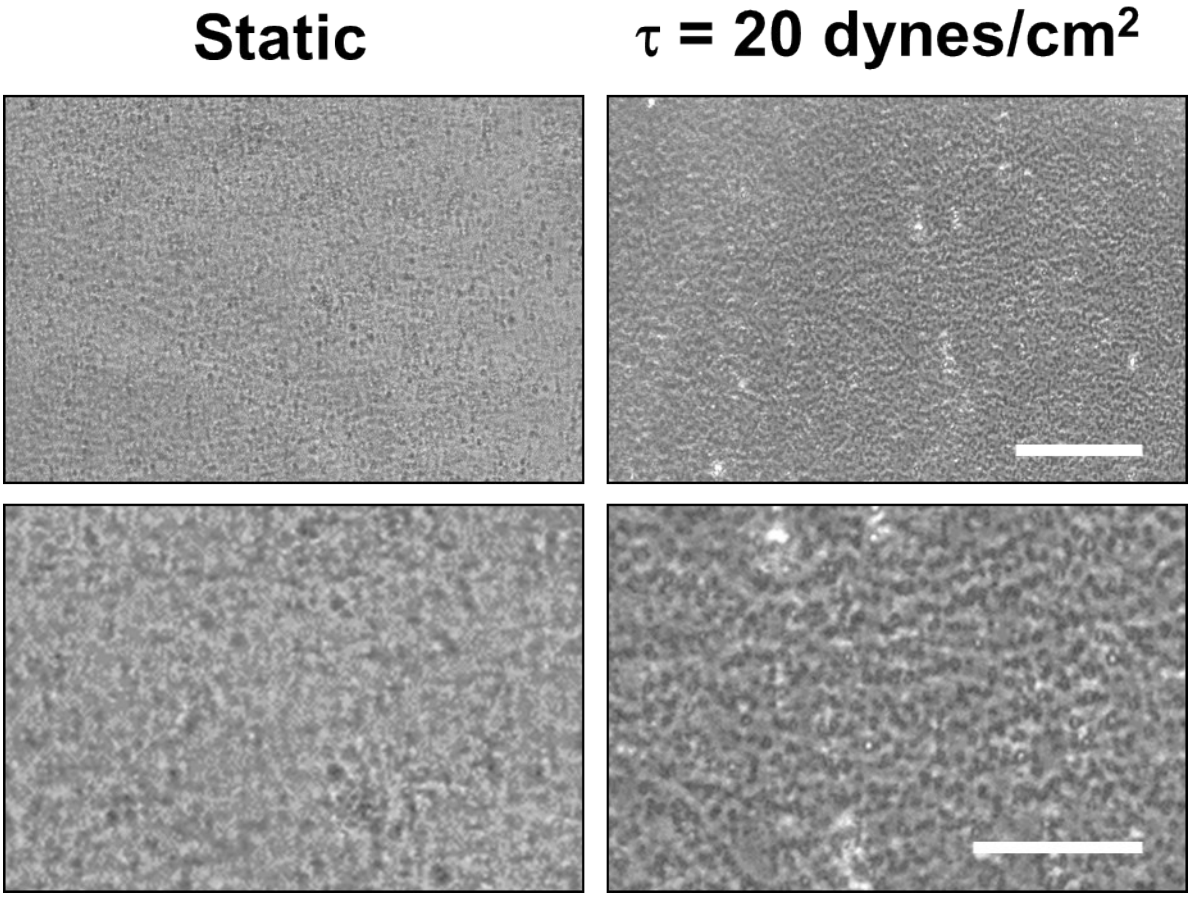

Supplementary Figure S10. Immobilized platelets remain attached to the bottom of the well surface after treatment with shear stress. To examine the stability of the platelets adhered to the bottom of the well plate, the well plates were treated with 0.5 dynes/cm^2 of shear stress for one hour followed by increasing bouts of shear stress up through 20 dynes/cm^2 for 5 minutes (mimicking experimental conditions) and visualized with phase contrast microscopy. Top bar =100 μm, bottom bar = 50 μm.

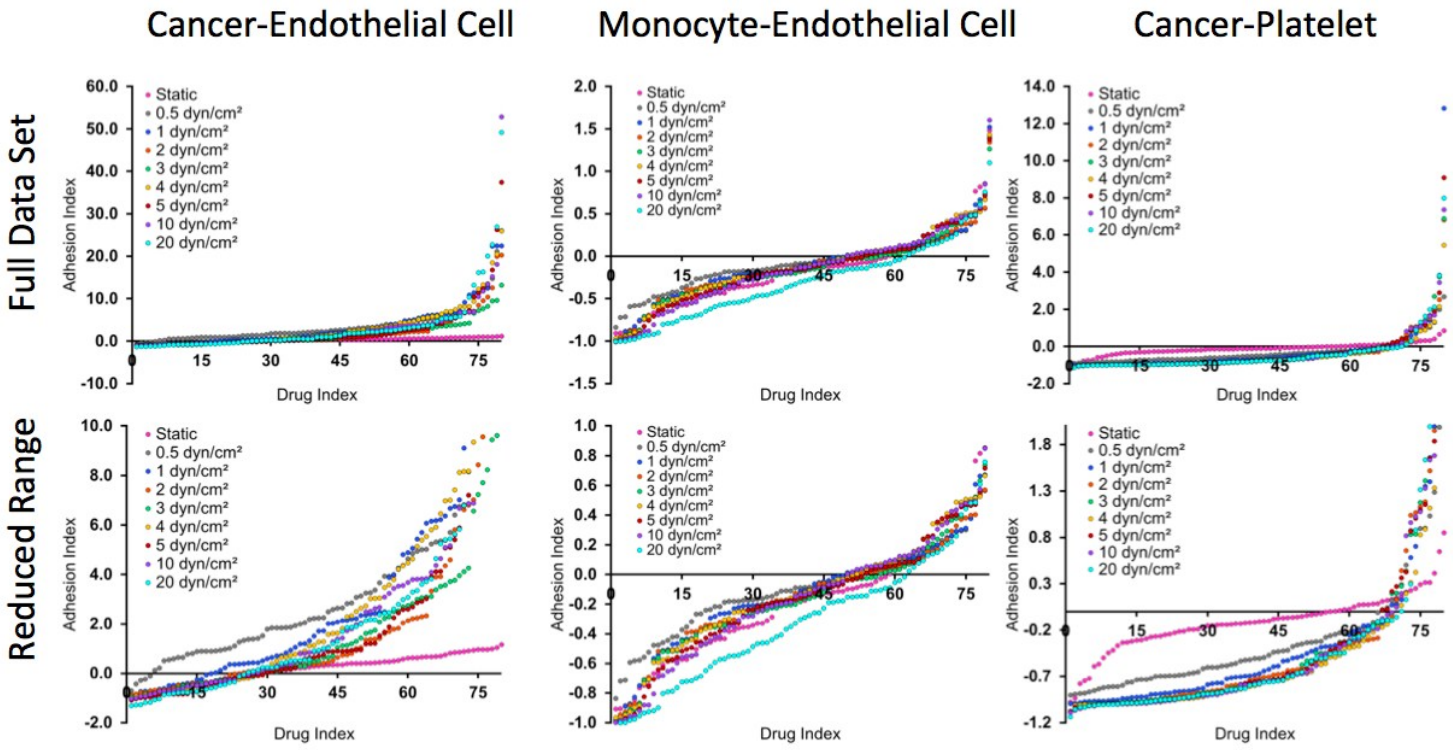

Supplementary Figure S11. Adhesion indices of kinase library drugs in rank order at increasing shear stresses for cancer and monocyte cell adhesion to endothelial cells and immobilized platelets. Kinase inhibitors were ranked in order of smallest to largest adhesion index for cell adhesion statically, under 0.5 dyn/cm^2 shear stress and for subsequent de-adhesion under increasing shear stresses ranging from 1 – 20 dyn/cm^2 after MDA-MB-231 breast cancer cells or THP-1 monocytes were treated with kinase inhibitors for one hour and then allowed to adhere to an activated endothelial cells or immobilized platelets, plotted over the entire data set, as well as over a reduced range on the y-axis.

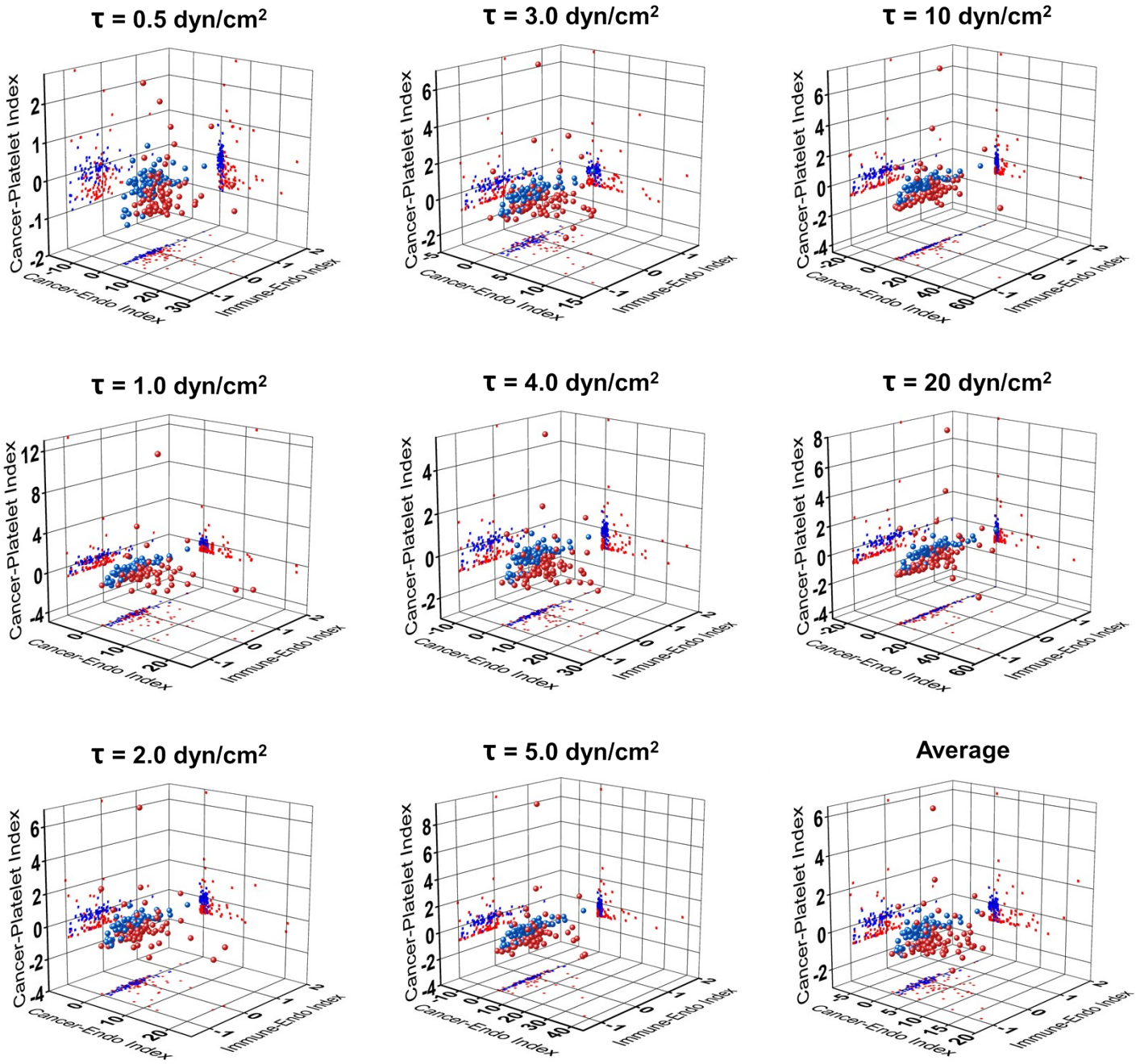

Supplementary Figure S12. 3-Dimensional plot of cancer-endothelial, cancer-platelet and immune endothelial adhesion indices from the kinase library screen with static and shear conditions. 3-Dimensional plots combining data from all three kinase inhibitor library screens including projections in each dimension for direction comparison between results between static adhesion and shear adhesion and deadhesion over shear stresses ranging from 1-20 dyn/cm^2 and an average adhesion index over the results from all of the shear stresses. Cancer and immune cells were treated for one hour and then adhered to endothelial cells or immobilized platelets for one hour before the deadhesion assay.

Supplemental Tables

Supplementary Table 1. Compounds included in the anti-inflammatory drug screen

Drug	Action	Conc. (μg/mL)	Conc. (mM)	Ref.
Aspirin	COX inhibitor	1000	5.55	(1)
Ibuprofen	COX inhibitor	500	2.42	(2)
Diclofenac	COX inhibitor	400	1.26	(3)
Prednisone	Glucocorticoid receptor agonist	50	0.14	(4)
Acetaminophen	COX-2 inhibitor	1000	6.62	(1)
Nicotine	Nicotinic receptor agonist	200	1.23	(5)
Furosemide	Loop diuretic	100	0.30	(6)
Amoxicillin	β-Lactam antibiotic	100	0.27	(7)

Supplementary Table 2. Compounds included in the anti-cancer drug screen

Drug	Action	Conc. (μg/mL)	Conc. (μM)	Ref.
Niclosamide	Uncouples oxidative phosphorylation	0.65	2	(8)
Marimastat	MMP inhibitor	3.31	10	(9)
GM6001	MMP inhibitor	3.89	10	(10)
Paclitaxel	Microtubule stabilizer	8.54	10	(11)
Doxorubicin	Topoisomerase II inhibitor	0.29	0.5	(12)
Erlotinib	Tyrosine kinase inhibitor	4.23	10	(13)
Fluorouracil	Thymidylate synthase	1.30	10	(14)

Supplementary Table 3. Compounds included in the integrin inhibitor drug screen

Drug	Action	Conc. (mg/mL)	Conc.	Ref.
P11	$\alpha_v\beta_3$/vitronectin inhibitor	0.018	25 nM	(15)
Cilengitide	$\alpha_v\beta_3$ and $\alpha_v\beta_5$ inhibitor	14.72	25 mM	(16)
ATN-161	$\alpha_5\beta_1$ inhibitor	29.86	50 mM	(17)
TC-I 15	$\alpha_2\beta_1$ inhibitor	1.06	2 mM	(18)
RGDS Peptides	Integrin inhibitor	43.34	100 mM	(19)
BIO 1211	$\alpha_4\beta_1$ inhibitor	0.0028	4 nM	(20)
Obtustatin	$\alpha_1\beta_1$ inhibitor	0.0088	2 nM	(21)
PF-562271	FAK inhibitor	6.65	10 mM	(22, 23)

Supplementary Table 4. Summary of results of integrin inhibitor screen. Compounds listed caused a significant reduction (>50%) in cancer cell adhesion to endothelial cells under the assay conditions.

Static Assay with MDA-MB-231 Cells		Static Assay with MCF-7 Cells	
Drug	**Action**	**Drug**	**Action**
None	N/A	P11	$\alpha_v\beta_3$/vitronectin inhibitor
		Cilengitide	$\alpha_v\beta_3$ and $\alpha_v\beta_5$ inhibitor
		BIO 1211	$\alpha_4\beta_1$ inhibitor
		Obtustatin	$\alpha_1\beta_1$ inhibitor
Shear Assay with MDA-MB-231 Cells		**Shear Assay with MCF-7 Cells**	
Cilengitide	$\alpha_v\beta_3$ and $\alpha_v\beta_5$ inhibitor	RGDS Peptide	Integrin inhibitor
ATN-161	$\alpha_5\beta_1$ inhibitor	BIO 1211	$\alpha_4\beta_1$ inhibitor
TC-I 15	$\alpha_2\beta_1$ inhibitor	Obtustatin	$\alpha_1\beta_1$ inhibitor
RGDS Peptide	Integrin inhibitor	PF-562271	FAK inhibitor
BIO 1211	$\alpha_4\beta_1$ inhibitor		
PF-562271	FAK inhibitor		

Supplementary Table 5. Hits from the kinase inhibitor library screen

Drug	Cancer-Endothelial Adhesion Index	Cancer-Platelet Adhesion Index	Monocyte-Endothelial Adhesion Index	CAS #
Akt Inhibitor IV	-0.679	-0.981	0.381	681281-88-9
Akt Inhibitor X	-0.537	-0.932	-0.339	925681-41-0
Flt-3 Inhibitor II	-0.839	-0.844	0.034	896138-40-2
Flt-3 Inhibitor III	-0.813	-0.984	-0.014	852045-46-6
PDGF Receptor, Tyrosine Kinase Inhibitor II	-0.514	-0.813	0.142	249762-74-1
PPI Analog II	-0.713	-0.844	-0.132	221244-14-0
Rapamycin	-0.555	-0.861	0.360	53123-88-9

Supplementary References

1. Pillinger MH*, et al.* (1998) Modes of action of aspirin-like drugs: salicylates inhibit erk activation and integrin-dependent neutrophil adhesion. *Proceedings of the National Academy of Sciences of the United States of America* 95(24):14540-14545.
2. Slater C & House SD (1993) Effects of nonsteroidal anti-inflammatory drugs on microvascular dynamics. *Microvascular research* 45(2):166-179.
3. Diaz-Gonzalez F*, et al.* (1995) Prevention of in vitro neutrophil-endothelial attachment through shedding of L-selectin by nonsteroidal antiinflammatory drugs. *The Journal of clinical investigation* 95(4):1756-1765.
4. MacGregor RR, Spagnuolo PJ, & Lentnek AL (1974) Inhibition of granulocyte adherence by ethanol, prednisone, and aspirin, measured with an assay system. *The New England journal of medicine* 291(13):642-646.
5. Speer P, Zhang Y, Gu Y, Lucas MJ, & Wang Y (2002) Effects of nicotine on intercellular adhesion molecule expression in endothelial cells and integrin expression in neutrophils in vitro. *American journal of obstetrics and gynecology* 186(3):551-556.
6. Wiemer G*, et al.* (1994) Furosemide enhances the release of endothelial kinins, nitric oxide and prostacyclin. *The Journal of pharmacology and experimental therapeutics* 271(3):1611-1615.
7. Hbabi L, Roques C, Michel G, Perruchet AM, & Benoist H (1993) In vitro stimulation of polymorphonuclear cell adhesion by ribomunyl and antibiotic + ribomunyl combinations: effects on CD18, CD35 and CD16 expression. *International journal of immunopharmacology* 15(2):163-173.
8. Osada T*, et al.* (2011) Antihelminth compound niclosamide downregulates Wnt signaling and elicits antitumor responses in tumors with activating APC mutations. *Cancer research* 71(12):4172-4182.
9. Hansen HP*, et al.* (2002) Inhibition of metalloproteinases enhances the internalization of anti-CD30 antibody Ki-3 and the cytotoxic activity of Ki-3 immunotoxin. *International journal of cancer. Journal international du cancer* 98(2):210-215.
10. Tremblay PL, Berthod F, Germain L, & Auger FA (2005) In vitro evaluation of the angiostatic potential of drugs using an endothelialized tissue-engineered

connective tissue. *The Journal of pharmacology and experimental therapeutics* 315(2):510-516.

11. Smitha KT*, et al.* (2013) In vitro evaluation of paclitaxel loaded amorphous chitin nanoparticles for colon cancer drug delivery. *Colloids and surfaces. B, Biointerfaces* 104:245-253.
12. Yang H, Filipovic Z, Brown D, Breit SN, & Vassilev LT (2003) Macrophage inhibitory cytokine-1: a novel biomarker for p53 pathway activation. *Molecular cancer therapeutics* 2(10):1023-1029.
13. Chen J*, et al.* (2011) The Bcl-2/Bcl-X(L)/Bcl-w inhibitor, navitoclax, enhances the activity of chemotherapeutic agents in vitro and in vivo. *Molecular cancer therapeutics* 10(12):2340-2349.
14. Grem JL, Mulcahy RT, Miller EM, Allegra CJ, & Fischer PH (1989) Interaction of deoxyuridine with fluorouracil and dipyridamole in a human colon cancer cell line. *Biochemical pharmacology* 38(1):51-59.
15. Lee Y, Kang DK, Chang SI, Han MH, & Kang IC (2004) High-throughput screening of novel peptide inhibitors of an integrin receptor from the hexapeptide library by using a protein microarray chip. *Journal of biomolecular screening* 9(8):687-694.
16. Taga T*, et al.* (2002) alpha v-Integrin antagonist EMD 121974 induces apoptosis in brain tumor cells growing on vitronectin and tenascin. *International journal of cancer. Journal international du cancer* 98(5):690-697.
17. Stoeltzing O*, et al.* (2003) Inhibition of integrin alpha5beta1 function with a small peptide (ATN-161) plus continuous 5-FU infusion reduces colorectal liver metastases and improves survival in mice. *International journal of cancer. Journal international du cancer* 104(4):496-503.
18. Miller MW*, et al.* (2009) Small-molecule inhibitors of integrin alpha2beta1 that prevent pathological thrombus formation via an allosteric mechanism. *Proceedings of the National Academy of Sciences of the United States of America* 106(3):719-724.
19. Moon C, Han JR, Park HJ, Hah JS, & Kang JL (2009) Synthetic RGDS peptide attenuates lipopolysaccharide-induced pulmonary inflammation by inhibiting integrin signaled MAP kinase pathways. *Respiratory research* 10:18.

20. Vanderslice P*, et al.* (2013) Small molecule agonist of very late antigen-4 (VLA-4) integrin induces progenitor cell adhesion. *The Journal of biological chemistry* 288(27):19414-19428.
21. Marcinkiewicz C*, et al.* (2003) Obtustatin: a potent selective inhibitor of alpha1beta1 integrin in vitro and angiogenesis in vivo. *Cancer research* 63(9):2020-2023.
22. Roberts WG*, et al.* (2008) Antitumor activity and pharmacology of a selective focal adhesion kinase inhibitor, PF-562,271. *Cancer research* 68(6):1935-1944.
23. Wiemer AJ*, et al.* (2013) The focal adhesion kinase inhibitor PF-562,271 impairs primary CD4+ T cell activation. *Biochemical pharmacology* 86(6):770-781.